Title
Different Gd3+ sites associated with magnetic ordering and structural distortions in Eu2CuO4:Gd3+ observed via electron-paramagnetic-resonance measurements.

Journal
Physical review. B, Condensed matter, 44(17)

ISSN
0163-1829

Authors
Zysler, RD
Tovar, M
Rettori, C
et al.

Publication Date
1991-11-01

DOI
10.1103/physrevb.44.9467

Different Gd^{3+} sites associated with magnetic ordering and structural distortions in Eu_2CuO_4:Gd^{3+} observed via electron-paramagnetic-resonance measurements

R. D. Zysler and M. Tovar*
Centro Atómico Bariloche and Instituto Balseiro, 8400 San Carlos de Bariloche, Río Negro, Argentina

C. Rettori,† D. Rao, H. Shore, and S. B. Oseroff
Physics Department, San Diego State University, San Diego, California 92182

D. C. Vier and S. Schultz
Physics Department, University of California, San Diego, La Jolla, California 92093

Z. Fisk
Los Alamos National Laboratory, Los Alamos, New Mexico 87545

S-W. Cheong
AT&T Bell Laboratories, Murray Hill, New Jersey 07974
(Received 25 March 1991; revised manuscript received 17 June 1991)

We have measured the EPR spectrum of dilute Gd^{3+} ions substituting for Eu^{3+} in Eu_2CuO_4. Each one of the resonance lines shows a splitting into two or more weaker lines below $T_N \approx 215$ K. The simultaneous appearance of a low-field microwave-absorption signal is attributed to the onset of long-range antiferromagnetic ordering with a weak ferromagnetic component. The splitting of the EPR spectrum is associated with different Gd sites in the magnetically ordered structure. A reduction of the local symmetry of the rare-earth sites below T_N is described in terms of an internal magnetic field lying in the *ab* plane and additional crystal-field terms related to local crystallographic distortions. Dipolar and exchange contributions to the internal field are discussed. Possible random static displacements of the oxygen atoms in the CuO_2 planes and their role in the development of the weak ferromagnetism and the presence of internal fields at the Gd sites are also analyzed. A strong dependence of the Gd EPR spectrum and the microwave absorption on the magnetic history of the samples has been observed, suggesting the formation of magnetic domains or a glassy state.

I. INTRODUCTION

The series of rare-earth cuprates $R_{2-x}(Ce, Th)_xCuO_4$ with (R = Pr, Nd, Sm, or Eu) show high-temperature superconductivity[1] at about 20 K, for $x \approx 0.15$. The study of these compounds presents particular interest because it has been proposed that the charge carriers involved in the superconductivity[2] are electrons, rather than holes as in the previously known high-T_c materials. They form, as do their parent compounds R_2CuO_4, in a tetragonal crystal structure[3] with CuO_2 planes in which oxygen atoms are square planar coordinated about the Cu atoms. Antiferromagnetic order of the Cu lattice has been detected by muon-spin rotation[4] and neutron-diffraction experiments[5–7] for $x = 0$, with R = Pr, Nd, and Sm. The Mössbauer spectra[8] of ^{57}Co ions doped into Eu_2CuO_4 indicates magnetic ordering of the Cu moments also in this material. A complex magnetic behavior[9] has been observed in compounds with heavier rare earths, such as Gd_2CuO_4, including the presence of weak ferromagnetism below 270 K. The measured ferromagnetic component in Gd_2CuO_4 and $(Eu,Gd)_2CuO_4$ solid solutions has been interpreted[10] as due to a combination of both a canting of the Cu moments away from perfect antiferromagnetism and a polarization of the paramagnetic Gd ions, which are coupled to the CuO_2 planes through an effective internal field of about 1 kG. Thus, it is of interest to analyze the microscopic interactions of dilute Gd^{3+} ions in $R_{2-x}Gd_xCuO_4$ in order to characterize their magnetic coupling to the Cu magnetic lattice.

In Ref. 11 we presented an electron-paramagnetic-resonance (EPR) study of Gd^{3+} in Eu_2CuO_4, where we analyzed the spectrum for the external magnetic field applied parallel to the c-axis of the tetragonal (T') crystal structure.[3] From the experimental data we determined the crystal-field parameters appropriate for the local symmetry, C_{4v}, of the Eu sites occupied substitutionally by the Gd atoms. A negative g shift was measured indicating exchange interactions with the host. We have also found recently that the EPR lines split when the magnetic field is oriented away from the c axis, and we tentatively associated this splitting with an internal magnetic field of dipolar origin.[12]

In this paper we report a detailed study of the angular dependence of the EPR spectra oriented towards a characterization of the internal magnetic field acting on the

Gd ions. In Sec. II we present the experimental data showing the following: (a) the angular dependence of the EPR spectra, (b) its temperature dependence, which suggests the presence of an internal field below a characteristic temperature, $T_0 \approx 215$ K (see the comment in Sec. II), and (c) the effects of the magnetic history of the sample, i.e., differences observed between cooling the sample through T_0 in zero applied magnetic field [zero-field cooled (ZFC)] or in a finite field [field cooled (FC)]. In Sec. III the data are analyzed in terms of a spin Hamiltonian, which includes the crystal-field interaction and an additional pseudo-Zeeman term, which takes into account the interaction with the effective internal field observed below T_0. The possibility of structural distortions is also discussed. Finally, the conclusions are presented in Sec. IV.

II. EXPERIMENTAL RESULTS

We have used single crystals of nominal composition $Eu_{1.99}Gd_{0.01}CuO_4$ grown in Pt crucibles using a flux technique.[13] Typical samples were thin platelets $3\times3\times0.1$ mm^9 in size. By x-ray fluorescence (XRF) analysis we have found that our crystals were contaminated by the presence of small amounts ($\approx 1\%$) of Pt. As it is almost certain that Pt replaces Cu in the CuO_2 antiferromagnetic planes, it may be the origin for the low measured value of T_0 (≈ 215 K). When crystals of Eu_2CuO_4:Gd were grown in alumina crucibles, values of $T_0 \approx 240$ K were obtained with no evidence of Al contamination. However, as the crystals grown in alumina crucibles were much smaller and the qualitative behavior was similar, we have used for this study only the crystals grown in Pt crucibles. The crystal structure is tetragonal[3] and the c axis is oriented perpendicular to the platelets. The measured lattice parameters[14] for pure Eu_2CuO_4 are $a = 3.910(1)$ Å and $c = 11.925(3)$ Å.

The EPR measurements were made with conventional spectrometers operating at X band and (9 GHz) and Q band (35 GHz), in the temperature range from 1.5 to 300 K.

A. Gd^{3+} single-ion EPR spectra

The measured spectrum of the Gd^{3+} dilute ions is shown in Fig. 1(a), for the external magnetic field, $\mathbf{H}_a$, applied parallel to the c axis. It corresponds to electronic transitions within the ground state ($4f^7;{}^8S_{7/2}$). The fine structure observed is comparatively simple for this orientation, and it has been analyzed in Ref. 11 in terms of a standard crystal-field Hamiltonian (see Sec. III A). The spectral lines are highly anisotropic, as we show in Figs. 2 and 3 for X band and $\mathbf{H}_a$ lying in the principal crystalographic planes (010) and (110), respectively, and in Fig. 4 for the Q band. The fine structure follows, in general, the angular dependence expected from the proposed crystal-field Hamiltonian (as it is discussed in Sec. III), but most of the resonance lines present an additional internal structure, which results in a splitting into two or more smaller lines. The magnitude of this splitting depends on (i) the orientation of the applied field with respect to the crystal axis, (ii) the electronic transition being observed, (iii) the magnetic history of the sample, and (iv) the temperature.

1. Angular dependence

As it is shown in Figs. 2–4, the splitting of each one of the resonance lines is observed when $\mathbf{H}_a$ is oriented away from the c axis, and it increases as a function of the angle, θ, between the c axis and $\mathbf{H}_a$. Because the total fine-structure splitting of the EPR spectrum is reduced as θ increases (and eventually the whole spectrum collapses at $\theta \approx 60°$), there is only a finite range where the splitting of the individual lines can be clearly resolved. For the Q band (see Fig. 4) this range extends up to $\theta \simeq 45°$, but for the X band (see Figs. 2 and 3) the experimental situation is more complex. For example, the $(+7/2 \leftrightarrow +5/2)$ transition, which shows the larger splitting, is also the weakest line and presents the largest crystal-field angular dependence, being superimposed on the $(+5/2 \leftrightarrow +3/2)$ transition at about $\theta \approx 15°$, the angle at which this latter transition starts to show a resolved splitting. Situations like this appear with other transitions, thus making difficult a detailed analysis at the X band, due to the uncertainty in identifying each of the superimposed spectral lines. For $\theta > 60°$ the spectra start to spread again at both

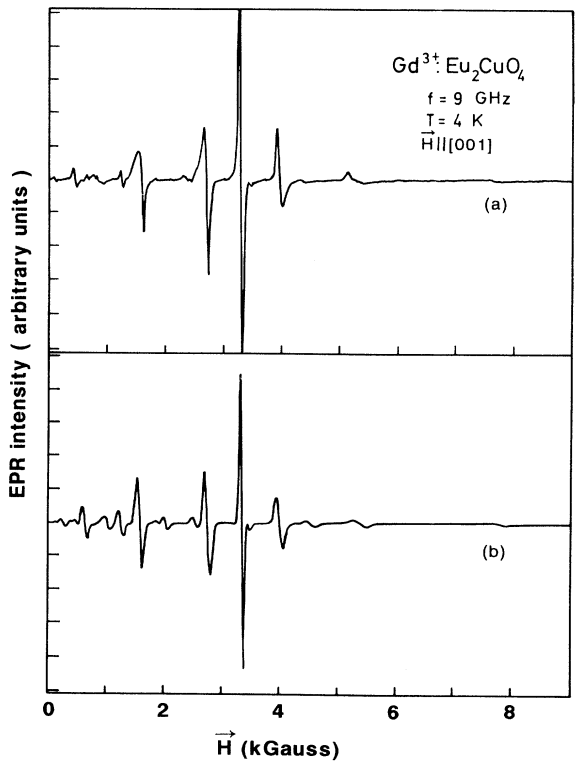

FIG. 1. X band EPR spectrum of Gd^{3+} in Eu_2CuO_4 with $\mathbf{H}_a \| c$-axis (a) measured at $T = 4$ K in a ZFC sample, (b) calculated with the crystal-field parameters of Table I. The "forbidden transitions" are included with their calculated relative intensity (see text).

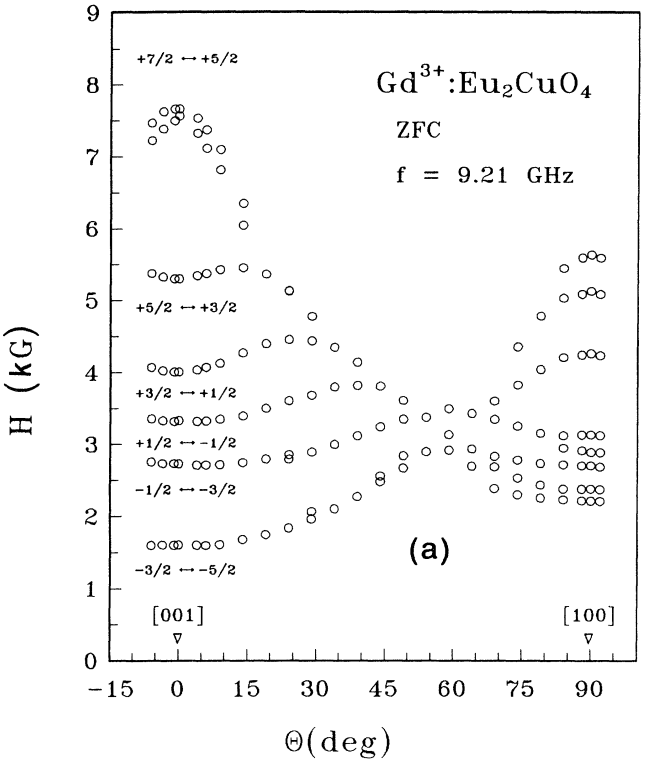

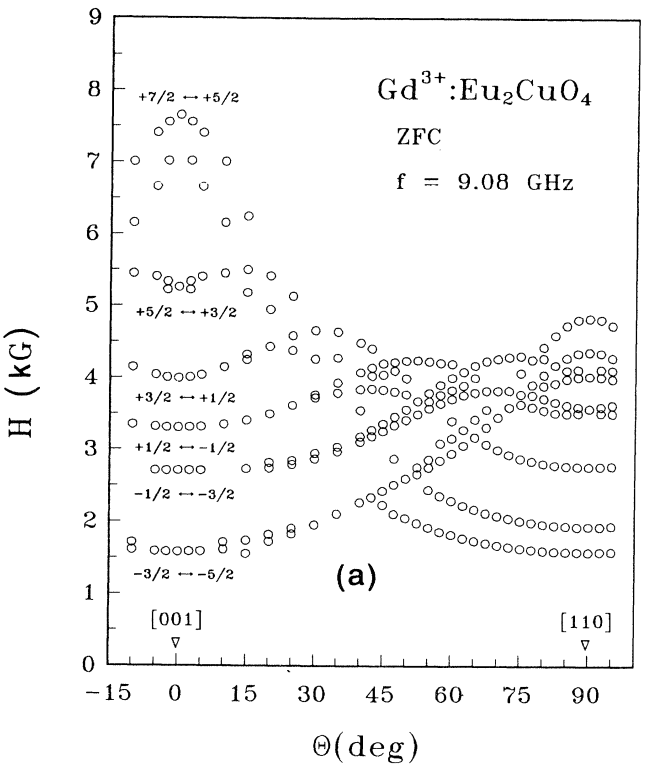

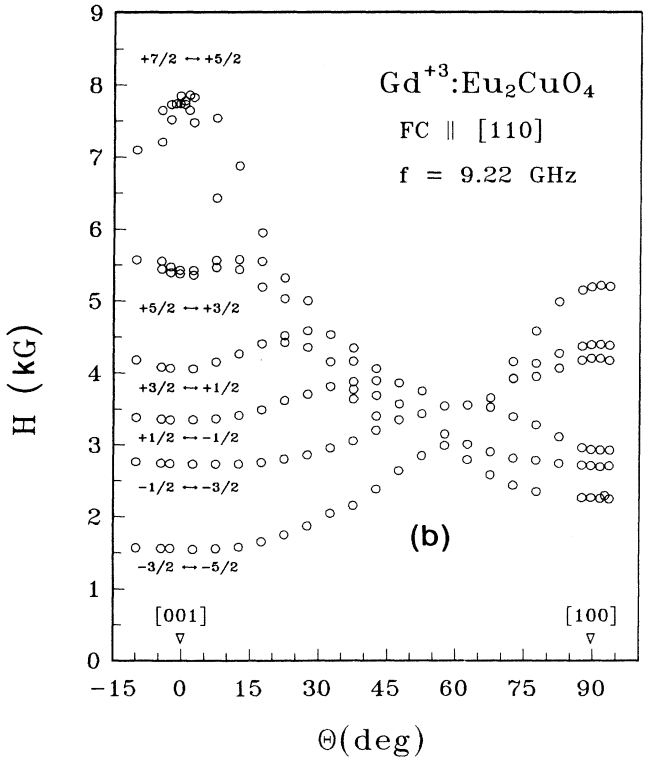

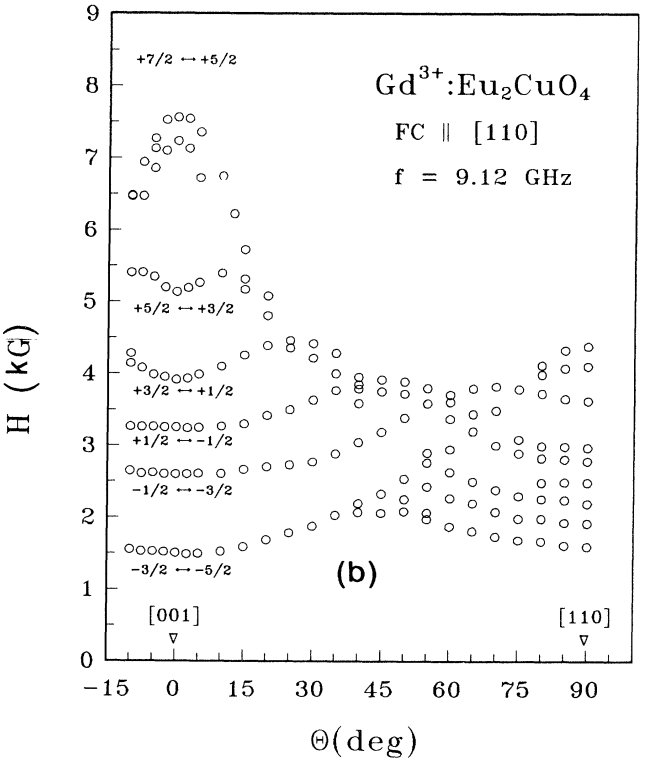

FIG. 2. Angular dependence of the 9 GHz Gd^{3+} EPR spectrum for the applied magnetic field oriented in the (010) plane: (a) ZFC and (b) FC in a field of 8-k G applied along [110].

FIG. 3. Angular dependence of the 9 GHz Gd^{3+} EPR spectrum for the applied magnetic field oriented in the $(1\bar{1}0)$ plane: (a) ZFC and (b) FC in a field of 15-k G applied along [110].

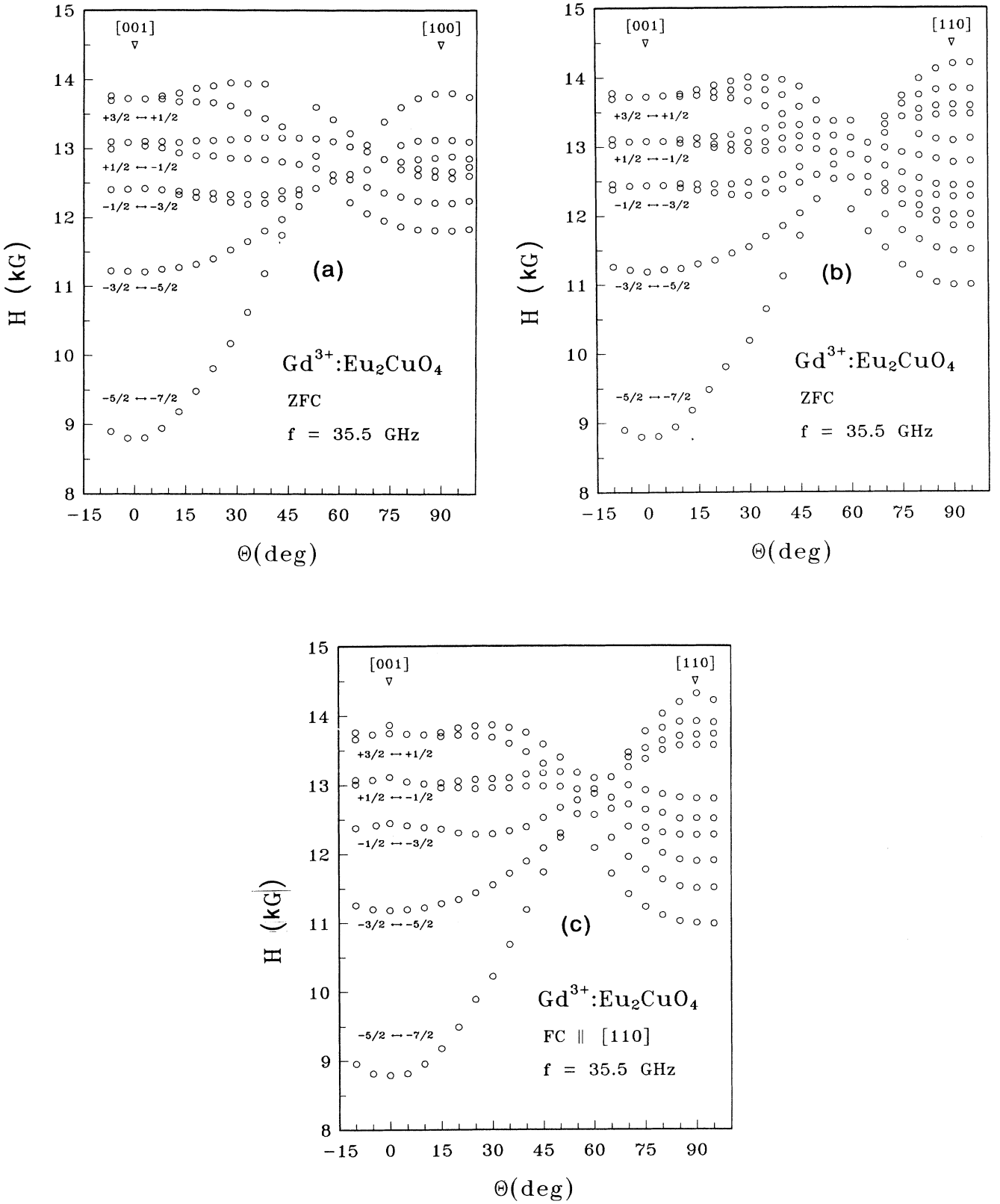

FIG. 4. Angular dependence of the 35 GHz Gd^{3+} EPR spectrum for the applied magnetic field, H_a, oriented (a) in the (010) plane (ZFC), (b) in the $(1\bar{1}0)$ plane (ZFC), and (c) in the $(1\bar{1}0)$ plane ($FC \| [110]$), with $H_c = 10$-k G.

frequencies, with a consequent gain in resolution for $\theta \approx \pi/2$. However, since for these angles the individual splittings are comparable to the fine-structure line separation, it is difficult to label *a priori* each line of the spectra. For these reasons we have centered the analysis of the data on the behavior of the Q band spectra in the angular range $0° \leq \theta \leq 45°$.

2. *Splitting of the different electronic transitions*

From the data in Fig. 4 it can be seen that for ZFC samples and $\mathbf{H}_a$ in the (010) plane, the $(+3/2 \leftrightarrow +1/2)$, $(+1/2 \leftrightarrow -1/2)$, and $(-1/2 \leftrightarrow -3/2)$ EPR lines split into weaker lines. A similar splitting is observed in the equivalent (100) plane. The relative ratio of the splitting for these three transitions is in a 3:2:1 approximate relation. The splitting of the remaining two observed lines, $(-3/2 \leftrightarrow -5/2)$ and $(-5/2 \leftrightarrow -7/2)$, is smaller than their measured linewidth ($\Delta H_{pp} \approx 100$ G).

For $\mathbf{H}_a$ in the (110) or $(1\bar{1}0)$ planes the $(+3/2 \leftrightarrow +1/2)$ and $(+1/2 \leftrightarrow -1/2)$ transitions clearly show a resolved splitting into three lines [Fig. 4(b)] instead of two [Fig. 4(a)], keeping approximately the same overall separation as in the (010) plane. However, the experimental resolution prevented the observation of this future splitting for the other transitions.

When measured at X band with $\mathbf{H}_a$ in the (110) or $(1\bar{1}0)$ planes, the resonance lines showed a splitting in ZFC samples, although the three lines could not be resolved as in the Q band. For $\mathbf{H}_a$ in the (010) and (100) planes the splitting was smaller than the linewidth and could not be measured.

3. *EPR spectra of ZFC and FC samples*

The magnitude of the splittings, as well as the relative intensity of each one of the split lines, was strongly dependent on the magnetic history of the sample, i.e, the way it was cooled through T_0. Although cooling the samples in a field parallel to the c axis had no effect on the spectra, important changes were observed when they were cooled in a field applied in the *ab* plane.

We present in Figs. 2(b), 3(b), and 4(c) the measured angular dependence of the X and Q band spectra for FC samples in magnetic fields varying from 8 to 15 kG and applied along the [110] axis, where the effects were largest. The measuring external field $\mathbf{H}_a$ was rotated from the [001] axis to the *ab* plane, along different crystallographic axes. The splitting of the Q band spectra in the (110) plane and near the c axis was reduced from three to only two lines, with the high-field line of the triplet being missed, as shown in Fig. 4(c). For the X band and $\mathbf{H}_a \| (110)$ intensity of some of the lines resonating at higher fields near the *ab* plane was reduced for FC samples. However, as stated previously, we could not identify the corresponding electronic transitions in this angular region. These effects showed no significant variations for the different cooling fields used. When the measuring field $\mathbf{H}_a$ was applied in the (100) or (010) planes, the effects of cooling in a field were less noticeable due to the smallness of the splittings compared to the linewidths.

For $\mathbf{H}_a$ oriented close to the *ab* plane, the differences between FC and ZFC samples were largest. The observed effects are illustrated in Fig. 5, where we display EPR spectra taken with the magnetic field applied along the [110] and [100] axes under different cooling conditions. Two extreme cases are shown: (a) sample cooled from room temperature to 4.2 K in zero applied magnetic field (ZFC) and the same sample cooled in a magnetic field of 15 kG applied parallel to the [110] axis. It is apparent from the figures that, although the general shape of the spectra remains approximately unchanged, the structure of such individual line is substantially modified. As can be observed, there is a complex behavior of the spectra showing not only changes in the relative intensity of the lines, but also shifts of their fields for resonance.

The angular dependence of the EPR spectrum has been measured in the *ab* plane, and it is interesting to point out that it shows 90° symmetry around the [001] axis for both ZFC and FC samples.

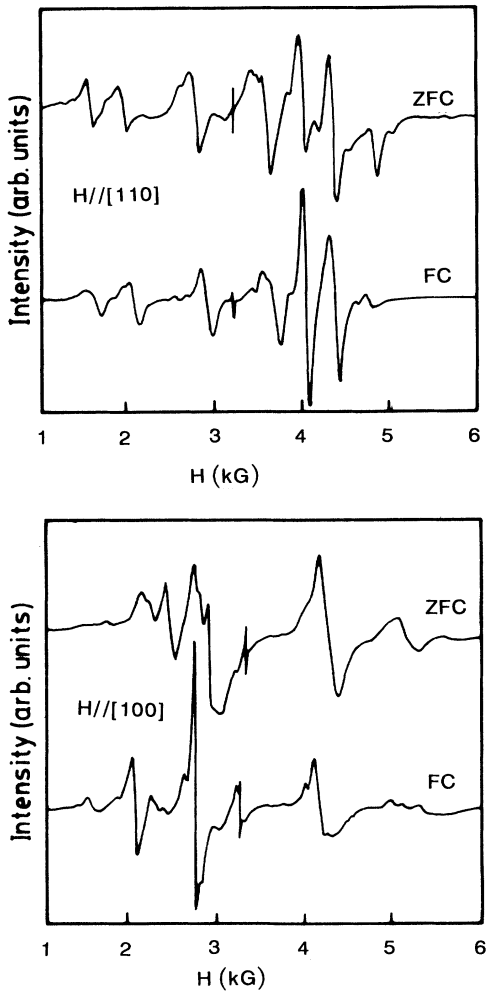

FIG. 5. EPR spectra measured at 9 GHz and $T=4.2$ K for samples: (a) ZFC and (b) FC in 15-k Gauss applied along [110]. The measuring field, H_a, was oriented along [110] and [100].

4. *Temperature dependence*

The EPR linewidth showed a large temperature dependence, as illustrated in Fig. 6 for the $1/2 \leftrightarrow -1/2$ transition with $\mathbf{H}_a \| c$ axis. Thus, it was necessary to choose particular orientations of the applied magnetic field in order to study the temperature dependence of the splitting of the EPR lines. In Fig. 7 we present a portion of a typical Q band spectrum showing the splitting of the resonance lines corresponding to the $(+3/2 \leftrightarrow +1/2)$ and $(+1/2 \leftrightarrow -1/2)$ electronic transitions, measured at 9 K with the magnetic field oriented 30° away from the c axis. Despite the strong increase of the peak-to-peak linewidth found above ≈ 60 K (indicated by vertical bars in Fig. 8), it is possible to observe that the individual splitting of these lines become smaller for increasing temperatures. As shown in Fig. 8, the splitting vanishes at about 200 K, when the characteristic temperature T_0 is approached. A similar temperature dependence has been observed for the splitting of the other electronic transitions.

B. Low-field absorption

For the magnetic field applied in the (001) plane we have observed microwave-absorption lines at low magnetic fields, as compared to the field for resonance at $g = 2$. This absorption presents a distinctive angular dependence, $H_r(\theta) = H_0/\sin\theta$, where θ is the angle between the applied magnetic field and the [001] axis and H_0 corresponds to the field for resonance when the applied magnetic field is in the (001) plane, i.e., parallel to the CuO_2 planes. The presence of these lines has already been reported in Ref. 9 as a signature of weak ferromagnetism for $(Eu_{1-x}Gd_x)_2CuO_4$, associated to a small canting of the Cu magnetic sublattices away from a perfect antiferromagnetic alignment. For Gd_2CuO_4 it has been determined[9,10] that the magnetic order is established below $T_N \approx 270$ K and for pure Eu_2CuO_4 the onset of weak ferromagnetism has been observed[9] at $T_N \approx 215(10)$ K.

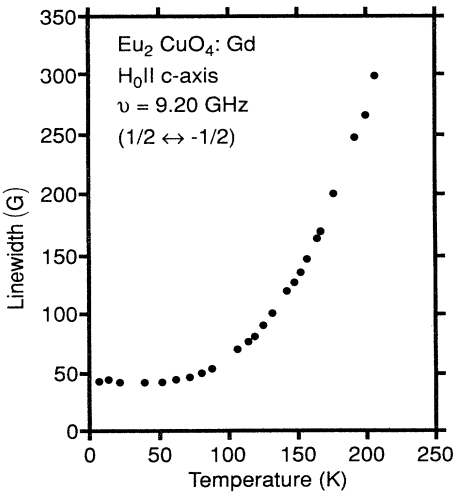

FIG. 6. Temperature dependence of the EPR linewidth for the $1/2 \leftrightarrow -1/2$ transition measured at 9.2 GHz with $\mathbf{H}_a \| c$ axis.

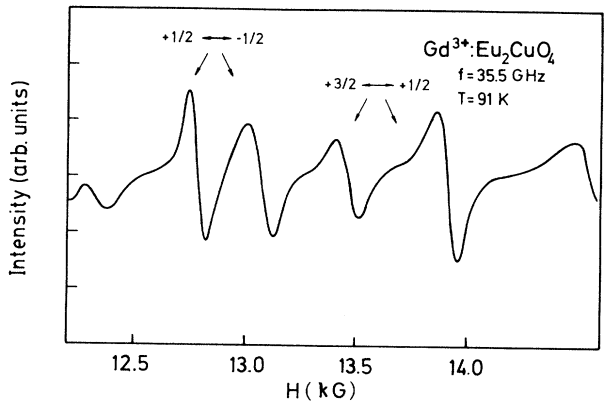

FIG. 7. Portion of the 35 GHz spectrum of Gd^{3+} taken at 91 K with the magnetic field lying in the (010) plane and oriented 30° away from the [001] axis, showing the splitting of the $(+3/2 \leftrightarrow +1/2)$ and $(+1/2 \leftrightarrow -1/2)$ transition lines. The sample was field cooled (FC) in a magnetic field of 15-k G along the [001] axis.

Details of this low-field resonance will be published elsewhere[15] but we want to emphasize here two characteristics observed for Eu_2CuO_4 and $Eu_{1.99}Gd_{0.01}CuO_4$, which are relevant to our analysis of the Gd^{3+} EPR spectra.

(i) The intensity of these lines is temperature dependent and decreases with increasing temperature, going to zero at about the same characteristic temperature, $T_0 \approx 210$ K, where the splitting of the Gd^{3+} EPR starts to develop.

(ii) The signal amplitude, relative to the intensity of the Gd^{3+} EPR lines, is strongly dependent on the magnetic

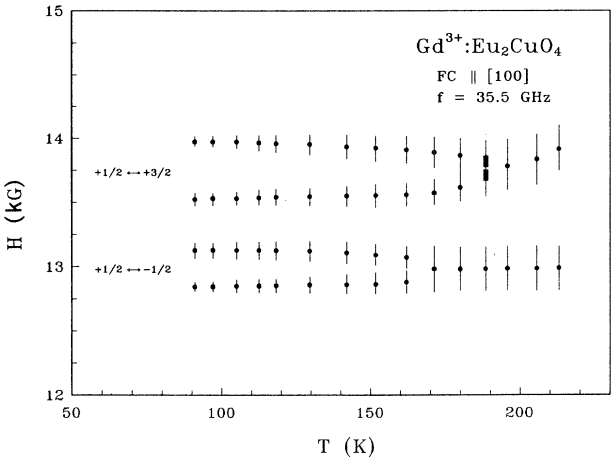

FIG. 8. Temperature dependence of the 35 GHz splitting for the $(+3/2 \leftrightarrow +1/2)$ and $(+1/2 \leftrightarrow -1/2)$ lines, measured with the magnetic field in the (010) plane and oriented 30° away from the [001] axis. The vertical bars indicate the measured peak-to-peak linewidths. The sample was cooled under the conditions indicated for Fig. 7.

history of the sample. The intensity is almost negligible for ZFC samples, and we have been able to detect a broad signal ($\Delta H_{pp} \approx 1000$ G) only through the use of special modulation techniques.[10] Instead, for samples FC in 15 kG, narrow lines ($\Delta H_{pp} \approx 50-100$ G) have been detected for $H \| [110]$ with an intensity much larger than that of the Gd^{3+} spectrum.

III. ANALYSIS OF THE EXPERIMENTAL DATA

A. Crystal-field Hamiltonian

The EPR spectrum has been described in Ref. 11 using a spin Hamiltonian appropriate for the tetragonal symmetry, C_{4v}, of the crystallographic site of the rare-earth ions in the unit cell:

$$\mathcal{H} = g_{\|}\mu_B H_z S_z + g_{\perp}\mu_B (H_x S_x + H_y S_y) + (b_2^0/3)O_2^0 + (b_4^0/60)O_4^0 + (b_4^4/60)O_4^4 , \quad (1)$$

where O_n^m are Stevens operators and b_n^m are the corresponding crystal-field parameters.

For the applied field oriented along the c axis, only the O_n^0 diagonal terms contribute, to first order, to the fine-structure splitting of the spectrum and the b_n^0 parameters can be determined directly from the EPR spectrum measured in this direction, as was done in Ref. 11. In that case, a rough estimate of the off-diagonal parameter b_4^4 was obtained from its second-order contribution to the measured fine structure of the spectrum for $H \| [001]$.

In this paper we have obtained more accurate values of the crystal-field parameters by taking into account the full angular dependence of the EPR spectrum. The parameters given in Table I were determined assuming the presence of an internal field, as discussed in Sec. III B.

The present results confirm the negative g shift reported in Ref. 11 for the magnetic field parallel to the c axis. The measured shift (with respect to the free ion value, $g = 1.991$) decreases with increasing temperature from $\Delta g = -0.058(3)$ at 1.5 K to $\Delta g = -0.040(3)$ at 200 K. At higher temperatures the individual linewidth increases very rapidly, thus preventing an accurate determination of the Hamiltonian parameters. As in the case[17] of Pr_2CuO_4:Gd, this broadening is probably due to relaxation via thermally populated excited electronic levels of the Eu^{3+} ions.[18] These levels may provide a channel for the relaxation of the dilute Gd^{3+} ions through an exchange or electric dipolar coupling mechanism.[17]

The EPR spectrum is more complex for the magnetic field oriented away from the c axis, because of the overlap of the resonance lines due to the decrease of the overall fine-structure spread of the spectrum and the splitting of the individual EPR lines. However, its average angular dependence (center of gravity of each electronic transition) is very well described by the crystal-field Hamiltonian of Eq. (1) with the parameters listed in Table I. The crystal-field parameters given in Table I were determined at 4.2 K and remained almost constant with temperature, within the experimental uncertainty.

TABLE I. Crystal-field parameters determined at 4.2 K for Gd^{3+} in Eu_2CuO_4.

$g_{\|}$	1.935(3)
b_2^0 (10^{-4} cm^{-1})	−513(4)
b_4^0 (10^{-4} cm^{-1})	−41(2)
$\|b_4^4\|$ (10^{-4} cm^{-1})	235(90)
$\|H_i\|$ (G)	350(50)

The total crystal-field energy represents ≈ 0.8 K, which is of the same order of magnitude as the Zeeman energy for the magnetic-field range of our experiments. For this reason the admixture of the Zeeman eigenfunctions through off-diagonal crystal-field terms is not negligible, and many EPR transition lines, usually forbidden under the selection rule $\Delta M = \pm 1$, become allowed with a significant transition probability, particularly for low applied fields ($H_a < 0.2T$), which is the range where a large number of "forbidden lines" has been observed at X band. We have compared the experimental data shown in Fig. 1(a) with the spectrum of Fig. 1(b), calculated with the crystal-field parameters given in Table I. The individual linewidths used for the calculation were taken from the measured spectrum, and the appropriate Boltzmann population factors have been included. The relative intensities are very sensitive to the magnitude of the off-diagonal terms in the Hamiltonian, and the good agreement obtained between the calculated and measured spectra is an indication of the internal consistency of the reported set of crystal-field parameters.

B. Internal magnetic field

The observation of a splitting of the spectral lines for the magnetic field oriented away from the [001] axis indicates the existence of nonequivalent sites occupied by the Gd^{3+} ions. The appearance of distinct sites for the Gd^{3+} ions in the crystal cell below T_0 may be attributed to magnetic ordering, a structural distortion, or a combination of both. For solid solutions of $Eu_{2-x}Gd_xCuO_4$, with $x \geq 0.20$, an effective field parallel to the ab plane has been determined[9,10] from measurements of dc magnetization. On the other hand, it has been suggested[10] that the tetragonal[3] $I4/mmm$ is only an average structure for Gd_2CuO_4, with either large thermal fluctuations or disordered static displacements of the oxygen atoms in the CuO planes, which reduce the local symmetry of the Gd sites. Finally, it should not be disregarded that there is the possibility of a simultaneous stabilization of this kind of distortion with the developing of weak ferromagnetism, which requires a reduction of the crystal symmetry.[9,10] From the analysis of the present EPR experiments we have found that the observed splittings can be described by adding extra crystal-field terms to the spin Hamiltonian of Eq. (1), which reflect the presence of local distortions (see Sec. III C) and a pseudo-Zeeman energy term associated with an internal magnetic field $\mathbf{H}_i$, lying in the ab plane. This pseudo-Zeeman term can be written as

$$\mathcal{H}_i = g_{\perp}\mu_B \mathbf{H}_i \cdot \mathbf{S} , \quad (2)$$

and affects the EPR spectrum in the following way: each Gd^{3+} ion "sees" a local field, $\mathbf{H}_{\rm loc} = \mathbf{H}_a + \mathbf{H}_i$, different in

magnitude from the applied field, $\mathbf{H}_a$, and also pointing in a direction generally not parallel to $\mathbf{H}_a$. The assumption of different local fields for each Gd site gives rise to a splitting of the spectral lines. The fact that the splitting appears below the same characteristic temperature, $T_0=215$ K, at which the low-field microwave absorption is first observed, strongly suggests that the origin of the internal field is associated with the magnetic ordering process of the Cu moments in the host lattice Eu_2CuO_4.

Eu_2CuO_4 is a Van Vleck paramagnet[18] as far as the magnetic behavior of the Eu ions is concerned. This fact is reflected in the temperature dependence of the EPR linewidths for the dilute Gd^{3+} ions (see Fig. 6). It is worth mentioning that, unlike other R_2CuO_4 compounds with magnetic ground states for the R^{3+} ions, the low-temperature narrowing due to the thermal depopulation of the excited states[17,18] has allowed this detailed study of the EPR line splitting. To our knowledge, the magnetic structure in Eu_2CuO_4 has not been determined yet. However, the appearance of signatures of weak ferromagnetism[9] in the microwave spectrum indicates the onset of magnetic order at ≈ 215 K. If we assume that this system presents a basic antiferromagnetic (AF) order with a magnetic configuration similar to that found in Nd_2CuO_4 (Ref. 5), Pr_2CuO_4 (Ref. 6), or Sm_2CuO_4 (Ref. 7), then the Eu sites in adjacent unit cells would be surrounded by reversed configurations of Cu moments, as it is illustrated in Fig. 9. These spin arrangements would create two

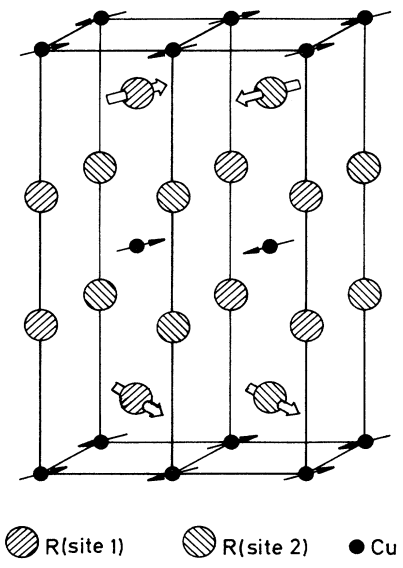

FIG. 9. Half magnetic cell illustrating the internal field orientation for the two nonequivalent Gd sites in two possible cases of magnetic coupling: (a) dipolar field with perfect antiferromagnetic alignment of the Cu sublattices (shown in the upper part of the cell), and (b) exchange coupling to a weak ferromagnetic component oriented perpendicular to the Cu lattice (shown in the lower part). Notice that the internal fields at neighboring Gd sites must point in opposite directions within a single AF domain in case (a), but not in case (b) where the orientation depends in the local canting of the Cu moments.

different sites in the magnetic structure with equal probability of occurrence. In addition, the possible existence of two kinds of magnetic domain[6] with orthogonal orientation of their magnetic moments should also be considered, taking into account that the weak anisotropy of the *dc* magnetization[9] in the *ab* plane supports the existence of these magnetic domains. Thus, for a general orientation of the external magnetic field each fine-structure line would split into four smaller lines, corresponding to the four possible orientations of the Cu moments surrounding each Gd ion. This argument remains valid either if Eu_2CuO_4 orders as Nd_2CuO_4 Pr_2CuO_4, or Sm_2CuO_4, since the main difference between the magnetic structures in these compounds lies in the orientation of the Cu moment at the center of the crystal unit cell with respect to those at the corners.

Within the hypothesis of perfect Af alignment we discuss two possible origins for the observed internal field at the Gd sites: (i) a classical dipolar magnetic field generated by the Cu moments[12] and (ii) a Heisenberg-type exchange coupling to the Cu moments. In the former case a calculation carried out assuming point dipoles[6] of $0.5\mu_B$ located at each Cu site, and adding the individual contributions from a sphere of 40 Å around the Gd site, gives a dipolar field $H_{\rm dip}\approx 470$ G. This value of $H_{\rm dip}$ is basically the same for the different magnetic structures of Pr_2CuO_4, Nd_2CuO_4, or Sm_2CuO_4. In all the cases considered, the dipolar field points in the $\langle 110\rangle$ directions (parallel to the Cu moments) with alternating signs in adjacent crystallographic unit cells, as indicated in Fig. 9.

If a scalar coupling of the type $\sum_k J_k \mathbf{S}_{\rm Gd}\cdot\mathbf{S}_{\rm Cu}^{(k)}$ is considered, the contributions from the four nearest neighbors cancel out when their moments show a perfect AF alignment. The main contribution should then come from second neighbors located along the c axis and will also be pointing along the $\langle 110\rangle$ directions, with alternating signs as in the case of the classical dipolar fields. Instead, when there is a canting of the Cu moments from the previously assumed perfect AF array, giving rise to a weak ferromagnetic component $\mathbf{M}_{\rm wf}$, a Heisenberg type of coupling between the Gd moments and their nearest Cu moments would no longer cancel, and a net interaction would be present. It can be described with an effective magnetic field parallel (or antiparallel) to the local contribution to $\mathbf{M}_{\rm wf}$ at each Gd site. From the *dc* magnetization measurements[10] in $Eu_{2-x}Gd_xCuO_4$, with $0.2\le x\le 2$, the presence of weak ferromagnetism has been inferred with $\mathbf{M}_{\rm wf}$ lying in the (001) plane. Although there is no experimental determination of the particular orientation of the microscopic contributions to $\mathbf{M}_{\rm wf}$ within this plane, it seems reasonable to assume them to be perpendicular to the Cu sublattice magnetization, i.e., along the $\langle 110\rangle$ directions. If so, the same four possible orientations of $\mathbf{H}_i$ within the *ab* plane would be present as in the cases previously analyzed.

Taking into account the symmetry of the system, all the split lines should collapse into a single one for $\mathbf{H}_a\|[001]$, since for this orientation all sites would be equivalent. Following the same line of reasoning the number of possible lines should also be reduced for certain orientations of the magnetic field when lying in crys-

tallographic planes of high symmetry. For example, the number of split lines should be two for $\mathbf{H}_a$ in the (100) and (010) planes and three for $\mathbf{H}_a$ in the (110) and (1$\bar{1}$0) planes. when $\mathbf{H}_a$ is in the (100) or (010) planes, perpendicular domains are equivalent and the spectrum of each transition should consist of two superimposed identical doublets (pairs of split lines). The two lines in the doublets are in correspondence with the two possible signs of the projection of $\mathbf{H}_i$ along $\mathbf{H}_a$ for the different Gd sites in each domain.

When $\mathbf{H}_a$ rotates in the (110) plane, the Gd sites in magnetic domains with effective fields $\mathbf{H}_i \| [1\bar{1}0]$ are still distinguishable, since their respective $\mathbf{H}_i$ are either parallel or antiparallel to $\mathbf{H}_a$, and the spectra of these sites should then give rise to doublets. Instead, the effective fields for the Gd sites of the domains pointing along [110] are orthogonal to $\mathbf{H}_a$, and should give rise to superimposed single resonance lines. An analogous situation occurs for $\mathbf{H}_a$ rotating in the (1$\bar{1}$0) plane. We expect then that in both cases each line splits into three weaker lines.

In the measured EPR spectrum for $\mathbf{H}_a \| [001]$ only unsplit lines appear, although they are somewhat distorted. This degeneracy indicates that for this orientation the angle between the applied, $\mathbf{H}_a$, and the local field, $\mathbf{H}_{\rm loc}$, is the same for all the Gd sites. This is consistent with our assumption of four different sites characterized by an internal field pointing in the [110], [1$\bar{1}$0], [$\bar{1}$10], and [$\bar{1}\,\bar{1}$0] directions, respectively. The distortion of the lines may be due to a small misorientation of the sample (less than 1°) or reflect inhomogeneous broadening arising from a small misalignment of the magnetic domains or a distribution of internal strains.

As we have indicated in Sec. II A, the spectral lines split when the field is oriented away from the [001] axis and the observed behavior is in qualitative agreement with the preceding analysis.

The $(+1/2 \leftrightarrow -1/2)$ transition is the least sensitive to changes in the crystal-field interaction (it is actually unaffected to first order in a perturbation scheme) and for this reason its splitting is expected to reflect mainly the effects of internal magnetic fields acting on the Gd site and not those resulting from small structural distortions. If the internal fields remain fixed to the ⟨110⟩ crystal axes, the total splitting of this line for H_a in the (110) plane, is given by

$$\delta H = 2H_i \sin\theta \tag{3a}$$

and corresponds to magnetic domains with $M_{\rm Cu}$ parallel to this plane. The lines associated with perpendicular domains would lie at an intermediate position. For $\mathbf{H}_a$ varying in the (100) plane the splitting is expected to be reduced to

$$\delta H = (2)^{1/2} H_i \sin\theta \ . \tag{3b}$$

From the splitting measured at the Q band for $0° < \theta \leq 45°$, and using expressions (3a) and (3b), we have determined the internal field H_i. Values of 350(50) G and 270(50) G were obtained from the data taken with $\mathbf{H}_a$ in the (100) and (110) planes, respectively. Internal fields of this magnitude are expected to produce a second-order shift of the fields for resonance when $\mathbf{H}_a \| [001]$. This effect should be particularly noticeable at the X band, where the applied fields are smaller than at the Q band. The intensity of the internal field H_i was then included as an extra parameter to be determined together with the crystal-field parameters. After a total diagonalization of the Hamiltonian, the best fitting of the X and Q band experimental data for $\mathbf{H}_a \| [001]$ gave a value of $H_i = 350(50)$ G for the internal field, in reasonable agreement with the values determined from the angular dependence of the splitting of the $(+1/2 \leftrightarrow -1/2)$ line.

Assuming internal fields of this magnitude and oriented in the four possible ⟨110⟩ directions, we have calculated the angular dependence presented in Figs. 10 and 11, which show a splitting of the lines as expected on symmetry grounds. For almost isotropic lines, such as the $(+3/2 \leftrightarrow +1/2)$, $(+1/2 \leftrightarrow -1/2)$, and $(-1/2 \leftrightarrow -3/2)$ at the Q band for $0° \leq \theta \leq 30°$, the total splitting is given approximately by Eqs. (3a) and (3b). Instead, as can be appreciated from Fig. 11, the splitting is slightly reduced for lines with a positive curvature in the angular dependence, such as the $(-3/2 \leftrightarrow -1/2)$ and $(-5/2 \leftrightarrow -7/2)$ transitions, and enlarged otherwise. This behavior results from the competition between the change in magnitude and relative orientation of the resulting local field with respect to the crystal axes.

The angular dependence of the Q band spectra obtained experimentally when cooling the system in zero field is consistent with the predicted behavior. This agreement, as far as the number of lines observed in each crystallographic plane and the angular dependence of the splitting are concerned, suggests that our assumption that the internal fields point in the four possible ⟨110⟩ directions is basically correct. However, the difference between the splittings measured for different electronic transitions is larger than predicted.

C. Structural distortions

As has been pointed out in Refs. 9 and 10, a structural distortion may be required in order to explain the weak ferromagnetic interactions observed in $Eu_{2-x}Gd_xCuO_4$. X-ray crystallographic studies[3,19] of Gd_2CuO_4 indicate an anomalously large thermal parameter for the oxygen atoms, O(2), in the CuO_2 square planar array, and it has been suggested[19] that the refined[3] $I4/mmm$ tetragonal structure is only an average structure for this compound, where the O(2) oxygen atoms present disordered static displacements of ≈ 0.18 Å along the [100] and [010] axes. If distortions of this kind are indeed present in Gd_2CuO_4 and they are related to its weak ferromagnetism, we can expect to find them also in the case of Gd-doped Eu_2CuO_4. Then, the local symmetry of the Gd sites should be reduced from C_{4v} to C_1, with the spin Hamiltonian including additional terms of the type

$$\mathcal{H}_d = b_2^1(c,s)O_2^1(c,s) + b_2^2(c,s)O_2^2(c,s) \ , \tag{4}$$

where c and s stand for linear combinations of Stevens operators, as defined in Ref. 20. For oxygen displacements given by $\varepsilon\mathbf{a}$ or $\eta\mathbf{b}$, with ε and η varying randomly

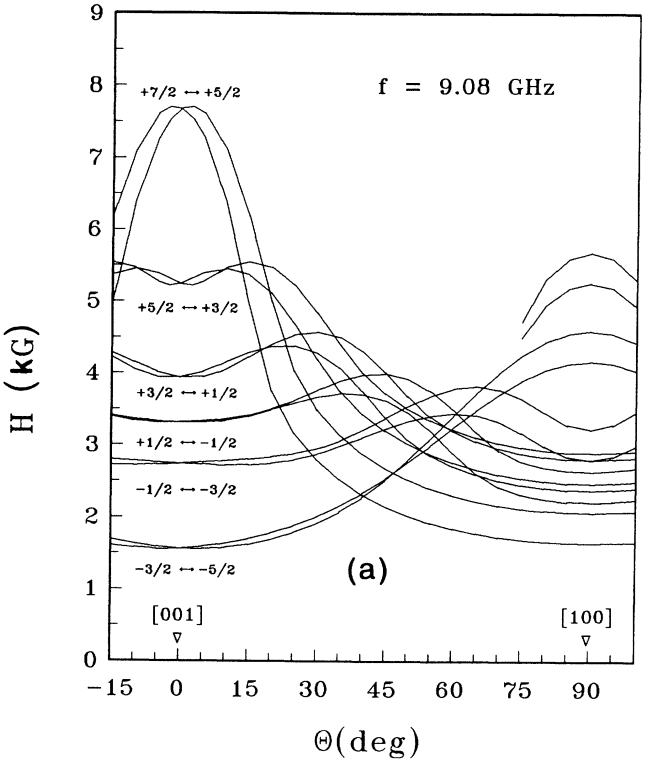

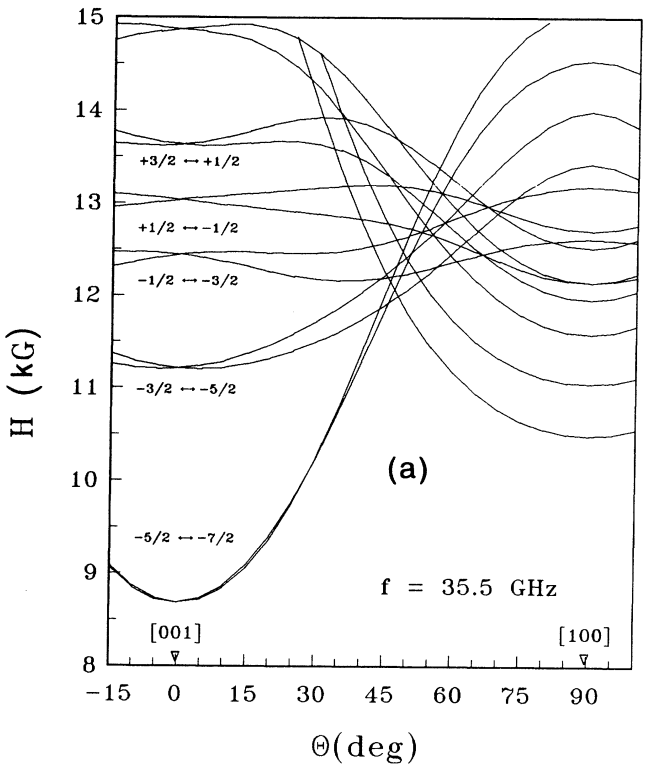

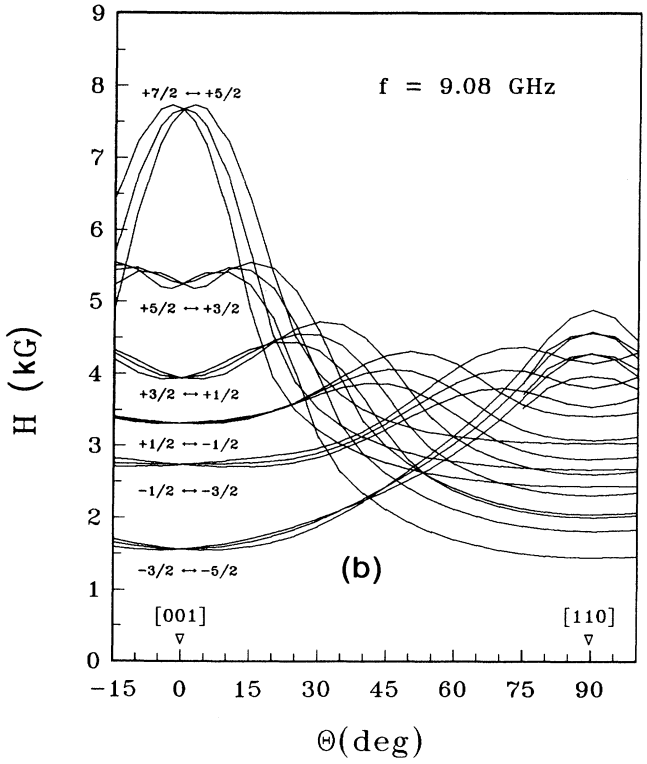

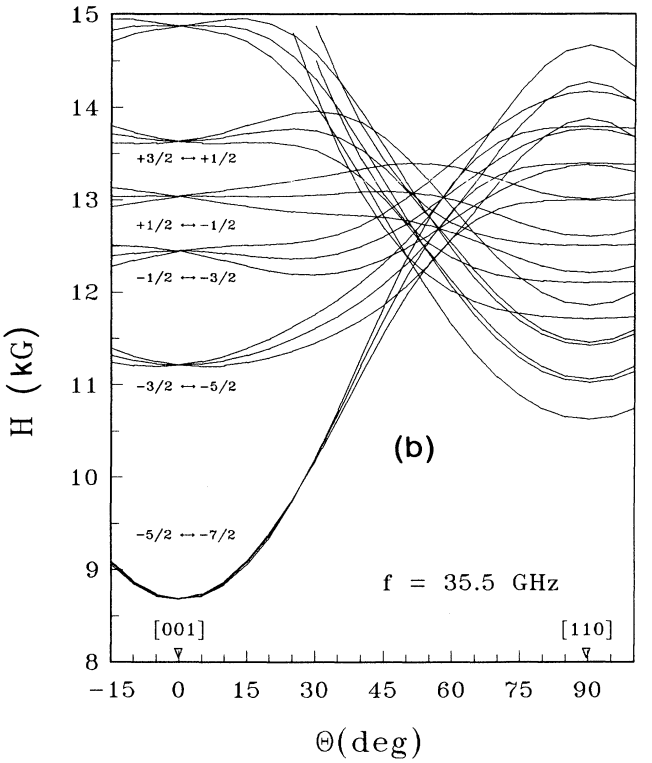

FIG. 10. Calculated angular dependence for the splitting of the 9 GHz spectrum for (a) H_a in the (010) and (b) in the $(1\bar{1}0)$ planes. An internal field of 350 G was included, pointing in the ⟨110⟩ directions. No structural distortions have been considered in the calculation.

FIG. 11. Calculated angular dependence of the splitting of the 35 GHz spectrum for (a) H_a in the (010) and (b) in the $(1\bar{1}0)$ planes. An internal field of 350 G was included, pointing in the ⟨110⟩ directions. No structural distortions have been considered in the calculation.

from site to site, the associated crystal-field parameters will change according to

$$b_2^1(c) \propto (\varepsilon+\varepsilon') ,$$

$$b_2^1(s) \propto (\eta+\eta') ,$$

$$b_2^2(c) \propto (\varepsilon-\varepsilon'-\eta+\eta') ,$$

$$b_2^2(s)=0 ,$$

where the displacements ε, ε', η, and η' are as indicated in Fig. 12.

For different orientations of the external magnetic field, this Hamiltonian can be expressed in a reference frame such that $z' \| \mathbf{H}_a$, and its diagonal part can be written as

$$\mathcal{H}' = D'(\theta,\phi) O_2^0(S') , \tag{5}$$

where $D'(\theta,\phi)$ may be obtained using the rotation rules given in Ref. 20.

Above T_0, our EPR data do not indicate any deviation of the crystal-field interaction from the proposed C_{4v} local symmetry within experimental uncertainty. Below T_0, where the splitting of the lines is observed, the local magnetic symmetry is reduced by the appearance of the internal field. Then, evidence of any structural distortion has to be deduced from the relative splitting measured for the different electronic transitions, through deviations from the calculated angular dependence on the basis of an internal field alone.

A detailed observation of the Q band splittings for the magnetic field applied away from the c axis and for $\theta < 45°$ indicates that the relative splitting of the transitions $(+3/2 \leftrightarrow +1/2)$, $(+1/2 \leftrightarrow -1/2)$, $(-1/2 \leftrightarrow -3/2)$, and $(-3/2 \leftrightarrow -5/2)$ can be better described by assuming that each doublet corresponds to a pair of Gd sites whose Hamiltonian includes, besides the effective magnetic field discussed in Sec. III B, an additional crystal-field term of the type given by Eq. (4). In order to analyze our data we have assumed that the contribution to the splitting due to local distortions may be described with effective parameters $\pm D'(\theta,\phi)$, where the + and − signs apply to each one of the two Gd sites in the doublet. We have found that $D'(\theta,\phi)$ increases almost linearly as a function of θ in the interval $20° < \theta < 45°$, for $\phi=0$ and $\phi=\pi/4$, i.e., for H_a varying in the (010) and (110) planes, respectively. The values of $D'(\theta,\phi)$ determined from the measurements in the these two planes are very similar and, for $\theta=\pi/4$, we obtained $D'(\pi/4,\phi) \simeq 30\times10^{-4}$ cm^{-1}. The observation of this crystal-field contribution to the measured splittings suggests that structural distortions accompany the developing of the internal fields below T_0. However, the experimental resolution did not allow a complete characterization of the angular dependence of $D'(\theta,\phi)$ and thus prevented a full determination of the crystal-field parameters in Eq. (4).

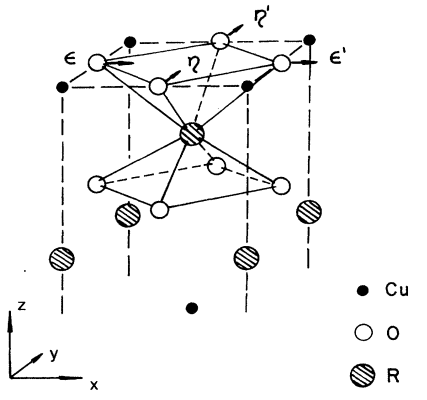

FIG. 12. Suggested environment of a Gd^{3+} ion in Eu_2CuO_4. The possible local structural distortions due to displacements of the oxygen atoms in the CuO_2 planes are shown.

D. Weak ferromagnetic domains

As we have pointed out in Sec. II, the measured EPR spectra is strongly dependent on the way the samples are cooled through T_0. Since our hypothesis is that the structure observed below T_0 corresponds to Gd sites in neighborhoods with different magnetic configurations, the changes observed for FC samples should be ascribed to field-induced modifications in the population of these sites or even changes in their local environment, as suggested by the shift of the field for resonance of the different lines. For instance, the disappearance at the Q band of the high-field line of each group for $\mathbf{H}_a$ in the $(1\bar{1}0)$ plane when cooling in a field $\mathbf{H}_c \| [110]$, may be interpreted as a preferential stabilization of the Gd sites with internal fields oriented in the direction of the field applied for cooling. This hypothesis of preferential orientation of microscopic domains is consistent with the observed narrowing of the low-field magnetoabsorption lines in FC samples, as compared to ZFC samples. It could also explain why the unusual microwave absorption observed[15] in FC samples of Eu_2CuO_4 has only been detected with the measuring magnetic field oriented perpendicular to the direction of the field for cooling.[15] However, the fact that the Gd^{3+} EPR spectrum presents 90° symmetry in the (001) plane for FC as well as ZFC samples, i.e., the spectrum is the same for H_a parallel, antiparallel, or perpendicular to H_c, indicates that the microscopic interpretation in terms of ferromagnetic domains is not straightforward. This observation raises a question: if we interpret the symmetry in the spectra of FC samples as a reversal or a rotation of the microscopic domains following the measuring field $\mathbf{H}_a$, why is it that we observe the different domains in the ZFC case without reorientation under the same applied fields?

IV. CONCLUSIONS

We have found in our experiments that the EPR spectrum of dilute Gd^{3+} ions substituting for Eu^{3+} ions in Eu_2CuO_4 is a sensitive probe of the local magnetic and structural changes that occur around the rare-earth sites. Each one of the resonance lines shows a splitting into two or more weaker lines at temperatures below $T_0 \approx 215(10)$

K. The simultaneous appearance at this temperature of a low-field microwave-absorption signal may be attributed to the onset of long-range magnetic order with a weak ferrromagnetic component. The splitting observed reflects then the existence of different Gd sites in the magnetically ordered structure. These sites present a point symmetry reduced from the C_{4v} symmetry attributed[3] to Eu^{3+} in Eu_2CuO_4.

Our analysis of the EPR data requires additional terms in the spin Hamiltonian in order to describe the angular dependence of the splittings that appear below T_0. These terms are (i) an internal magnetic field lying in the *ab* plane and (ii) crystal-field term associated with local distortions around the Gd^{3+} ions.

We have analyzed two possible mechanisms leading to the presence of an internal field at the Gd sites: dipolar and exchange interactions with the Cu moments. A dipolar magnetic field of 470 G has been calculated under the assumption of point magnetic dipoles of $0.5\mu_B$ located at the Cu sites and antiferromagnetically aligned. Although this value is close to the measured internal field, the fact that we did not observe it[18] in Pr_2CuO_4:Gd, suggests that (i) a different mechanism might be responsible for the internal field observed in the case of Eu_2CuO_4:Gd or (ii) this other mechanism competes with the dipolar field in such a way that the total field cancels in Pr_2CuO_4:Gd.

The exchange coupling of Gd ions to the magnetic moments of their four nearest Cu neighbors cancels exactly for a perfect AF order and only the interaction with next nearest neighbors is not compensated. In this case the comparison with Pr_2CuO_4:Gd^{3+} leads to the same conclusions as in the case of a dipolar field. However, we should notice that, while it is possible[18] to fit the EPR spectrum of Gd in Pr_2CuO_4 by assuming C_{4v} symmetry at the Gd site both above and below T_N, additional crystal-field terms, which reduce the point symmetry, need to be included in order to describe the angular variation of the EPR spectra in the case of Eu_2CuO_4. The reduction in the local symmetry could give rise to a nonperfect AF ordering resulting in a weak ferromagnetic component, an assumption that is supported by the low-field magnetoabsortion[9] present in Eu_2CuO_4 but not observed in Pr_2CuO_4. A canting of the Cu moments could in turn lift the frustration of the exchange interaction between the Gd ions and their nearest Cu planes, being in this way responsible for the internal field observed below T_N in the EPR spectrum of Gd^{3+} in Eu_2CuO_4 and not seen in Pr_2CuO_4. The strong dependence of the Gd^{3+} EPR spectra and the low-field magnetoabsortion on the magnetic history of the sample may be taken as evidence of the formation of metastable states in Eu_2CuO_4 below T_N, which could be associated with the formation of macroscopic magnetic domains or some sort of glassy state.

ACKNOWLEDGMENTS

This research was partially supported at the Centro Atómico Bariloche by the Consejo Nacional de Investigaciones Científicas y Técnicas de la República Argentina, at San Diego State University by the National Science Foundation (NSF) under Grant Nos. NSF-DMR-88-01317 and NSF-INT-89-00851, at the University of California, San Diego by Grant Nos. NSF-DMR-86-13858 and ONR-N00014-87-K-03381, and the work performed at Los Alamos National Laboratory was supported in part by the United States Department of Energy. One of the authors (M.T.) acknowledges partial support from the Fundación Antorchas (Argentina) and the Dirección General de Investigación Cientifica y Técnica del Ministerio de Educación y Ciencia de España.

*Present address: Instituto de Ciencia de Materiales de Barcelona, CSIC, Campus UAB, 08193 Bellaterra, Spain.

†Permanent address: Instituto de Física, UNICAMP, 13081 Campinas (SP), Brazil.

[1]Y. Tokura, H. Takagi, and S. Uchida, Nature (London) **337**, 345 (1989); H. Takagi, S. Uchida, and Y. Tokura, Phys. Rev. Lett. **62**, 1197 (1989); J. T. Markert and M. B. Maple, Solid State Commun. **70**, 145 (1989); J. T. Markert, E. A. Early, T. Bjorholm, S. Ghamathy, B. W. Lee, J. J. Neumeier, R. D. Price, C. L. Seaman, and M. B. Maple, Physica C **158**, 178 (1989).

[2]J. M. Tranquada, S. M. Heald, A. R. Moodenbaugh, G. Liang, and M. Croft, Nature (London) **337**, 720 (1989).

[3]Hk. Müller-Buschbaum, and W. Wollshcläger, Z. Anorg. Allg. Chem. **414**, 76 (1975); B. Grande, Hk. Müller-Buschbaum, and M. Suhweizer, *ibid.* **428**, 120 (1977); Kimberly A. Kubat-Martin, Z. Fisk, and R. R. Ryan, Acta Crystallogr. C **44**, 1518 (1988).

[4]G. M. Luke, B. J. Sternlieb, Y. J. Uemura, J. H. Brewer, R. Kadono, R. F. Kiefl, S. R. Krtizman, T. M. Riseman, J. Gopalakrishnan, A. W. Sleight, M. A. Subramanian, S. Uchida, H. Takagiana, and Y. Tokura, Nature (London) **338**, 49 (1989).

[5]P. Allenspach, S.-W. Cheong, A. Dommann, P. Fischer, Z. Fisk, A. Furrer, H. R. Ott, and B. Rupp, Z. Phys. B **77**, 185 (1989); H. Yoshizawa, S. Mitsuda, H. Mori, Y. Yamada, T. Kobayashi, H. Sawa, and J. Akimitsu, J. Phys. Soc. Jpn. **59**, 428 (1990).

[6]J. Akimitsu, H. Sawa, T. Kobayashi, H. Fujiki, and Y. Yamada, J. Phys. Soc. Jpn. **58**, 2646 (1989); Y. Endoh, M. Matsuda, K. Yamada, K. Kakurai, Y. Hidaka, G. Shirane, and R. J. Birgeneau, Phys. Rev. B **40**, 7023 (1989); D. C. Cox, A. I. Goldman, M. A. Subramanian, J. Gopalakrishnan, and A. W. Sleight, *ibid.* **40**, 6998 (1989).

[7]S. Skanthakumar, J. W. Lynn, J. L. Peng, and Z. Y. Li, J. Appl. Phys. **69**, 4866 (1991).

[8]S. Jha, D. Suyanto, R. Hogg, G. M. Julian, R. A. Dunlap, S-W. Cheong, Z. Fisk, and J. D. Thompson, Hyperfine Interact. **61**, 1143 (1990).

[9]S. B. Oseroff, D. Rao, F. Wright, M. Tovar, D. C. Vier, S. Schultz, J. D. Thompson, Z. Fisk, and S-W. Cheong, Solid State Commun. **70**, 1159 (1989); S. B. Oseroff, D. Rao, F.

Wright, D. C. Vier, S. Schultz, J. D. Thompson, Z. Fisk, S-W. Cheong, M. F. Hundley, and M. Tovar, Phys. Rev. B **41**, 1934 (1990).

[10]J. D. Thompson, S-W. Cheong, S. E. Brown, Z. Fisk, S. B. Oseroff, M. Tovar, D. C. Vier, and S. Schultz, Phys. Rev. B **39**, 6660 (1989).

[11]D. Rao, M. Tovar, S. B. Oseroff, D. C. Vier, S. Schultz, J. D. Thompson, S-W. Cheong, and Z. Fisk, Phys. Rev. B **38**, 8920 (1988).

[12]R. D. Zysler, M.Tovar, S. B. Oseroff, D. C. Vier, S. Schultz, Z. Fisk, and S-W. Cheong, Bull. Am. Phys. Soc. **35**, 429 (1990).

[13]K. A. Kubat-Martin, Z. Fisk, and R. R. Ryan, Acta Crystallogr. C **44**, 1518 (1988).

[14]Kimberly A. Kubat-Martin, and R. R. Ryan (private communication).

[15]D. C. Vier, S. Schultz, C. Rettori, D. Rao, S. B. Oseroff, M. Tovar, Z. Fisk, and S-W. Cheong, J. Appl. Phys. **69**, 4872 (1991).

[16]We have used angular modulation of the static field through the application of a modulation field perpendicular to the external field, a technique described by E. Edgar, J. Phys. E **8**, 179 (1975).

[17]C. Rettori, D. Rao, S. Oseroff, R. D. Zysler, M. Tovar, Z. Fisk, S-W. Cheong, S. Schultz, and D. C. Vier, Phys. Rev. B **44**, 826 (1991).

[18]M. Tovar, D. Rao, J. Barnett, S. B. Oseroff, J. D. Thompson, S-W. Cheong, Z. Fisk, D. C. Vier, and S. Schultz, Phys. Rev. B **39**, 2661 (1991).

[19]Ph. Galez, P. Schweiss, G. Collin, and R. Bellissent, J. Less Common Met. **164&165**, 784 (1990).

[20]M. T. Hutchings, in *Solid State Physics,* edited by F. Seitz and D. Turnbull (Academic, New York, 1964), Vol. 16.